# Stability of Droplets Suddenly Exposed to a High Velocity Gas Stream

**FREDERICK C. HAAS**

**Cornell Aeronautical Laboratory, Inc., Buffalo, New York**

This paper considers the breakup of droplets suddenly exposed to a high velocity air stream. Consider a globule of liquid material exposed to a gas stream in such a manner that a velocity differential exists between the liquid and the gas. The gas flowing over the surface of the liquid globule causes the pressure normal to the surface of the body to be nonuniform, resulting in a distortion of the liquid body. If the pressure forces cause a distortion severe enough to overcome the surface tension and viscous forces within the liquid, the liquid globule will break. Because a balance of forces is involved, there is a body size above which all globules will break under influence of specific environmental conditions, and below which none will break when acted upon by identical environmental conditions. The largest sized body that will not break is designated as the critical sized body. This paper considers the critical sized body, the time required for breakup of bodies larger than critical size, and the distortion of the body during breakup, for a spherical body instantaneously exposed to a gas stream of constant velocity with respect to time. Such conditions are encountered when melting occurs in a high speed environment or after disintegration of liquid jets introduced into a high gas velocity environment.

Application of dimensional analysis to the general problem results in three important dimensionless terms: Weber number $\frac{R \rho_g V^2}{\sigma_l}$, the ratio of dynamic pressure forces to the surface tension forces, gas phase Reynolds number $\frac{\rho_g V R}{\mu_g}$, and a viscosity group $\frac{\mu_l^2}{R \sigma_l \rho_l}$, containing only properties of the liquid. A qualitative analysis of the globule splitting mechanism cited in reference *1* leads to similar dimensionless groups. The Reynolds number of the system implicitly defines the pressure distribution on the surface of the globule. This paper considers the laminar boundary layer flow region, $1{,}000 < N_{Re_D} < 200{,}000$ for flow over a sphere. The flow region where viscous forces become important with respect to inertial forces, $N_{Re_D} = 10$, is considered in a preliminary manner.

Hinze (*1*) reasons that liquid viscosity retards deformation; hence the critical Weber number for highly viscous liquids may be written in the functional relationship:

$$N_{We_{c_\mu}} = N_{We_{c_{\mu=0}}} \left[1 + f\left(\frac{\mu_l^2}{R \sigma_l \rho_l}\right)\right] \qquad (1)$$

The viscosity group may be ignored for many liquid materials, and accordingly this paper considers only the case $\mu_l^2 << R \sigma_l \rho_l$.

## DEFORMATION OF LIQUID GLOBULE

The deformation of a liquid globule under the influence of nonuniform pressure distribution was formulated by Hinze (*2*). For materials of slight viscosity effect ($\mu_l^2 << R \sigma_l \rho_l$), instantaneously exposed to a constant speed high velocity gas stream, deformation of the stagnation point region is given by

$$\left.\frac{\delta}{R}\right|_s = N_{We} \sum_n \frac{C_n}{2(n-1)(n+2)} (1 - \cos \omega_n t) \qquad (2)$$

where

$$\omega_n^2 = n(n-1)(n+2) \frac{\sigma_l}{\rho_l R^3} \qquad (2a)$$

and $C_n$ represents the constants obtained when the pressure distribution on the sphere is expanded in a series of zonal surface harmonics of the form

$$\frac{P(\phi)}{P(0)} = \sum_n C_n P_n (\cos \phi) \qquad (2b)$$

The general zonal surface harmonic $P_n(\beta)$ of order $n$ is given in reference *4*.

The experimentally measured pressure distribution on a sphere, as given by Flashsbart (*5*), has been utilized, in this work, as the driving force for deformation. This pressure distribution, somewhat different from the approximated pressure distribution used by Hinze (*3*), leads to considerably different critical criteria for the deformation of a breaking droplet. The actual experimental pressure distribution takes the series form

$$\frac{P(\phi)}{P(0)} = \sum_n C_n P_n (\cos \phi) = -0.282 + 0.282 P_1 (\cos \phi) + 0.454 P_2 (\cos \phi) + 0.430 P_3 (\cos \phi) + 0.188 P_4 (\cos \phi) - 0.023 P_5 (\cos \phi) - 0.045 P_6 (\cos \phi) \qquad (3)$$

Substitution into Equation (2) in terms of $\omega_2 t$ yields

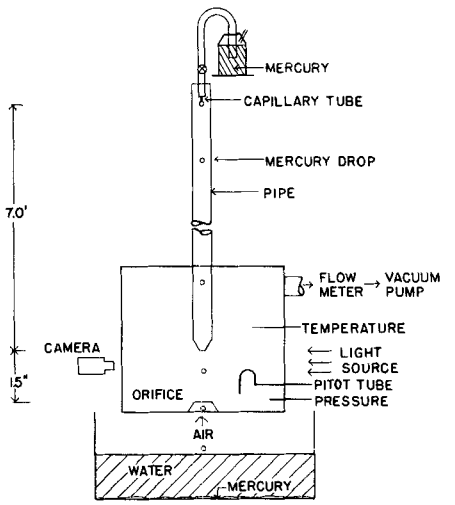


Fig. 1. Experimental apparatus.

F. C. Haas is now with the West Virginia Pulp and Paper Company, Luke, Maryland.

$$\frac{\delta/R|_s}{N_{We}} = 0.0566\,(1-\cos\omega_2 t) + 0.0217\,(1-\cos 1.94\,\omega_2 t)$$
$$+ 0.0052\,(1-\cos\omega_3 t) - 0.00041\,(1-\cos 4.2\,\omega_3 t)$$
$$- 0.00056\,(1-\cos 5.48\,\omega_3 t) \quad (4)$$

This equation is maximized with respect to $\omega_2 t$ at a value of approximately $0.83\pi$. The maximum deformation allowed by Equation (2) is given as

$$\frac{\delta/R|_{s_m}}{N_{We_c}} = 0.13 \quad (5)$$

The time required to reach maximum deformation is given directly by the maximized value of $\omega_2 t$:

$$t_{s_m} = 0.92\frac{R}{V}\sqrt{\frac{\rho_l}{\rho_g}N_{We_c}} = 2.55\frac{R}{V}\sqrt{\frac{\rho_l}{\rho_g}\delta/R|_{s_m}} \quad (6)$$

Equations (5) and (6) describe the ability of a drop to break based on the Weber number, the maximum displacement of the stagnation point surface, and the time required for deformation to reach the maximum value. The critical Weber number was determined by experiment, and on this basis the maximum distortion and time to reach maximum distortion were computed and compared with observed experimental values.

## EXPERIMENTAL MEASUREMENTS

The experimental program was concerned with the region of pressure distribution corresponding to $N_{Re_D} > 1{,}000$ and liquids for which $\mu_l^2 << R\sigma_1\rho_l$. The liquid studied was mercury. The experimental apparatus is shown in Figure 1. Drops of mercury formed on the tip of a capillary tube were allowed to fall freely through a long tube which was sealed to gas flow. The high velocity gas stream was formed by aspirating air through a ¼-in. orifice. Gas velocity in the test section was measured with a pilot tube. The center core of the orifice flow was essentially at constant velocity for a distance of 1 in. above the orifice. The drop entered this core and was acted upon by the high velocity gas. The action was recorded with two high-speed movie cameras (6,000 frames/sec.) taking pictures at points 90 deg. apart. Gas density was computed from test chamber temperature and pressure. Precaution was taken to prevent velocity pulsations and vibrations in the apparatus. Drop radius was taken as a mean spherical value as calculated from the measured weight of fifty drops. In nearly all cases this compared favorably with the value measured on the photographs. Surface tension data were taken from the literature. Triple-distilled mercury was used in all experiments. Time measurements were obtained from the camera framing rate measured at the time the photographs were taken.

Data were taken by selecting the capillary tube which gave the desired diameter drop. Globule dropping rate and gas flow were adjusted to the desired rate. After equilibrium conditions (temperature and pressure) were established, photographs of the action were taken. The motion pictures were projected upon a screen and data taken by a frame-by-frame analysis of the breakup action. Only drops that fell through the center core to the gas jet were studied in order that deviations between local and mean gas velocity, for the zone of interaction with the liquid, were held to a minimum. The transition from stagnant gas conditions to high velocity gas conditions ($V_g >> -V_l$) was not instantaneous; however, analysis of photographic data indicated that a very small portion of the liquid drop deformation occurs in this region.

The data concerning breakup of the globules are shown in Table 1. These data were obtained with mercury drops breaking in air at a pressure slightly less than 1 atm. and temperature ranging between 70° and 75°F. Exact measured values of temperature and pressure were used in the calculations of $N_{We}$ and $N_{Re}$ listed in Table 1. Breakup of the drop was observed in all tests with Weber number equal to and greater than 6.0. In all tests with Weber number less than 5.2 breakup was not observed. Information was not obtained in the interval between 5.2 and 6.0, for the purpose of future calculations the critical Weber number is taken to be 5.6.

In all observations of Weber number between 6 and 30 the mechanism of deformation and breakup was similar. The drop enters the high velocity gas stream as a sphere. The sphere initially becomes deformed at the front surface. The front surface becomes flattened and the rear surface remains spherical; the original sphere becomes a hemisphere. As the process continues, the droplet becomes very thin and flat, taking the shape of a wafer. Thereafter, the drop expands in the planes parallel and normal to the direction of gas flow into a bag shaped body with a heavy ring of material at the edge of the original wafer. The bag is composed of a very thin film of material attached to a ring which contains a large portion of the total mass of material. After the bag becomes inflated, the top surface rips out of the bag and the thin film of material which composed the bag forms into small droplets. The heavy ring of material at the base of the bag breaks into many droplets; however, the resulting droplets are much larger than those formed by the film. In all tests, the largest droplet formed on breakup was smaller than the critical size droplet corresponding to the environmental conditions. The phenomenon of breakup from a bag formation is similar to that observed under other circumstances in references 6 and 7.

Figures 2 through 5 show the various stages of deformation for a typical breakup in the range $5.6 < N_{We} < 30$. The photographs show four of thirty-four frames of the breakup sequence for a droplet at $N_{We} = 15.5$. The mercury globule is falling vertically, and gas flow is upward in the vertical direction. Figure 2 shows the initial droplet deformation to a hemispherical shape. Figure 3 shows the wafer shaped deformation. In all observations of droplet breakup it was noted that after the deformation reached the wafer shape, further deformation was delayed for a period of time. During this time there was no detectable change in appearance or size of the wafer shape. Figure 4 shows the droplet at one stage of the bag formation process. The thin wafer expands in directions parallel and normal to the direction of gas flow and begins to form a bag of thin film liquid attached to a ring which contains a major portion of the liquid. Figure 5 shows the globule an instant after the top of the bag has torn. This is the beginning of globule disintegration into small droplets.

It was observed in the experiments that the breakup mechanism at Weber numbers five to six times greater than critical value is different from the mechanism observed near the critical condition. At Weber numbers greater than 30 the breakup appears more chaotic, and the formation of a thin film bag is not obvious.

Equation (5) relates the critical Weber number to a maximum deformation of the globules. When one uses the experi-

TABLE 1. STABILITY DATA FOR MERCURY DROPS

| $D$ (in.) | $V$ (ft./sec.) | $N_{We}$ | $N_{Re}$ | Breakup |
|---|---|---|---|---|
| 0.083 | 118 | 3.36 | 2,450 | No |
| 0.083 | 420 | 34.4 | 8,800 | Yes |
| 0.080 | 255 | 14.3 | 5,350 | Yes |
| 0.075 | 235 | 11.1 | 4,500 | Yes |
| 0.024 | 235 | 3.63 | 1,440 | No |
| 0.078 | 270 | 15.5 | 5,500 | Yes |
| 0.056 | 380 | 22.2 | 5,500 | Yes |
| 0.080 | 414 | 37.5 | 8,700 | Yes |
| 0.028 | 344 | 8.95 | 2,500 | Yes |
| 0.037 | 344 | 11.90 | 3,300 | Yes |
| 0.048 | 280 | 10.28 | 3,500 | Yes |
| 0.032 | 241 | 5.10 | 2,000 | Yes |
| 0.027 | 241 | 4.20 | 1,700 | No |
| 0.060 | 216 | 7.62 | 3,380 | Yes |
| 0.036 | 216 | 4.58 | 2,025 | No |
| 0.060 | 198 | 6.40 | 3,100 | Yes |
| 0.044 | 198 | 4.70 | 2,360 | No |
| 0.062 | 188 | 6.00 | 3,040 | Yes |
| 0.054 | 188 | 5.20 | 2,650 | No |

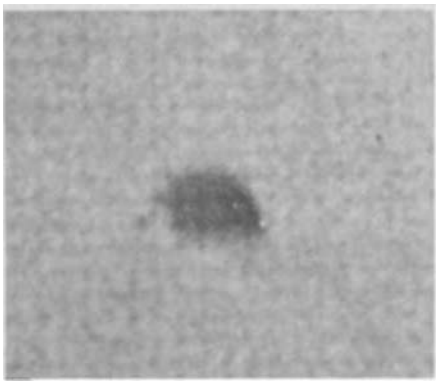

Fig. 2. Photograph of mercury droplet deformed to hemispherical shape ($N_{We} = 15.5$, $t = 1.6$ msec.).

mentally developed critical Weber number of 5.6, Equation (5) indicates a maximum deformation:

$$\delta/R|_{s_m} = 0.72 \tag{7}$$

The time required for maximum deformation of the globule is given by Equation (6). Substituting the maximum deformation value of 0.72 one obtains

$$t_{s_m} = 2.17 \frac{R}{V} \sqrt{\frac{\rho_l}{\rho_g}} \tag{8}$$

## DISCUSSION OF BREAKUP MECHANISM

The mechanism of breakup observed includes deformation of the sphere to a thin wafer, formation of an inverted bag, and a final bursting of the thin film which makes up the bag. The droplet deformation model formulated by Hinze indicates that a maximum deformation must occur. Comparison of experimental results with predictions based on the model indicates that this deformation corresponds to the formation of a thin wafer shaped body. Figure 6 shows the time required for formation of the thin wafer as a function of the parameter $\frac{R}{V}\sqrt{\frac{\rho_l}{\rho_g}}$ which becomes evident from Equation (6). Equation (8) is also shown on Figure 6. Equation (8), developed by combination of analysis and experimental observation of the critical Weber number, shows reasonable agreement with the experimentally determined data for time of formation to the thin wafer shape.

Measurements of the deformation of mercury droplets to a wafer shape are shown in Figure 7. Equation (7) indicates the maximum deformation occurs at a $\delta/R|_{s_m}$ value of 0.72. The average value of $\delta/R|_{s_m}$ from the experiments is 0.66. These measurements provide reasonable confirmation of the analytical result, considering the experimental inaccuracies in accessing the wafer thickness.

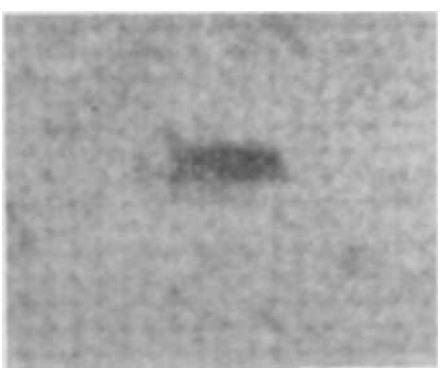

Fig. 3. Photograph of mercury droplet deformed to thin wafer shape ($N_{We} = 15.5$, $t = 2.6$ msec.).

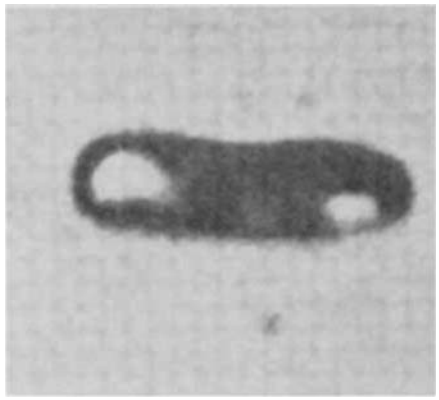

Fig. 4. Photograph of mercury droplet during bag formation process ($N_{We} = 15.5$, $t = 5.0$ msec.).

Deformation of nonbreaking drops did not proceed to the thin wafer shape; however, some deformation of the sphere was noted. For drops that did not break, the deformation varied from 0.12 to 0.46. Sufficient data were not taken to determine a correlation with Weber number.

Figure 8 shows the experimentally determined time for start of bag formation and the time required for total breakup of the globule as a function of $\frac{R}{V}\sqrt{\frac{\rho_l}{\rho_g}}$. The difference in time between the start of bag formation (Figure 8) and the wafer formation (Figure 6) corresponds to the apparent secession of deformation cited previously. All time measurements were made by considering the globule entry into the high velocity gas stream as zero time. Total breakup was interpreted as the point where the material had completely broken into small droplets.

## PRELIMINARY ANALYSIS OF BREAKUP AT LOW REYNOLDS NUMBER

In connection with small drops acted upon by a high velocity gas stream it is of interest to estimate the effects of low Reynolds number. At these conditions the pressure distribution on the body and the stagnation pressure change due to the increasing effects of ambient fluid viscosity. The deformation model developed by Hinze (2) assumes that tangential forces are small compared with normal forces. A conservative preliminary estimate of the effects of low Reynolds number is developed by considering the effects of stagnation pressure and pressure distribution changes caused by the viscous effects of the ambient fluid. Jensen (8) presents the pressure distribution on spheres at various low Reynolds numbers, while Homann (9) presents the stagnation point effect. For Reynolds number of 10 the pressure distribution in zonal surface harmonics takes the form

Fig. 5. Photograph of mercury droplet after inflated bag has torn ($N_{We} = 15.5$, $t = 6.0$ msec.).

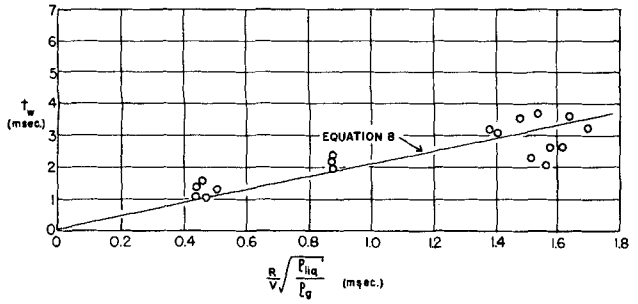


Fig. 6. Experimentally determined time for thin wafer formation.

$$\frac{P(\phi)}{P(0)} = -0.158 + 0.663\,P_1(\cos\phi) + 0.434\,P_2(\cos\phi) + 0.042\,P_3(\cos\phi) + 0.015\,P_4(\cos\phi) - 0.009\,P_5(\cos\phi) + 0.002\,P_6(\cos\phi) \quad (9)$$

This pressure distribution yields the following equation for the maximum deformation:

$$\frac{\delta/R|_{sm}}{N_{We}\left[1 + \dfrac{12}{N_{Re_D} + 0.643\sqrt{N_{Re_D}}}\right]} = 0.11 \quad (10)$$

For $N_{Re_D} = 10$ this equation becomes

$$\frac{\delta/R|_{sm}}{N_{We_c}} = 0.214$$

Comparison with Equation (5) indicates that the criterion for maximum deformation changes by approximately 60% because of the increased pressure and changed pressure distribution caused by the ambient viscous effect.

For the low Reynolds number conditions the time required to reach maximum deformation is given by

$$t_{sm} = 3.33\frac{R}{V}\sqrt{\frac{\rho_l}{\rho_g}\frac{\delta/R|_{sm}}{\left[1 + \dfrac{12}{N_{Re_D} + 0.643\sqrt{N_{Re_D}}}\right]}} \quad (11)$$

which for $N_{Re_D} = 10$ becomes

$$t_{sm} = 2.38\frac{R}{V}\sqrt{\frac{\rho_l}{\rho_g}\delta/R|_{sm}} \quad (12)$$

Comparison with Equation (6) indicates that the changed pressure conditions cause a slower deformation. Equal deformation ratios are reached in a 10% longer time under the $N_{Re_D} = 10$ condition. These results are conservative and can only be considered preliminary because tangential forces introduced by the ambient viscous forces are not considered.

## SUMMARY

A study of the stability of liquid globules suddenly exposed to a high velocity gas stream has been carried out. Photographs of drop breakup indicate that disintegration of a globule under environmental conditions in the vicinity of critical conditions takes place in four distinct phases. The drop becomes deformed to a thin wafer shaped body of specific size; the wafer shaped body remains at constant size and shape for a period of time; the wafer forms into an inverted bag with a heavy ring of material at the base of the bag; and the bag finally breaks into a large number of droplets, the largest droplets being formed from the heavy ring of material. Combination of the experimental and analytical results indicates that the maximum deformation required for droplet breakup is the formation of a thin wafer shaped globule.

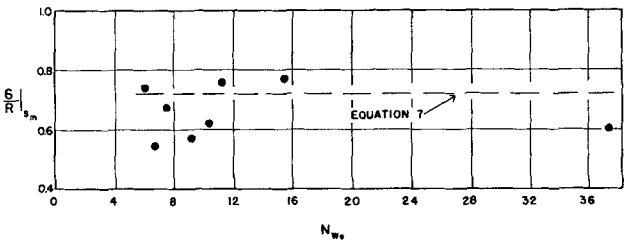


Fig. 7. Experimentally determined values of droplet deformation at time of thin wafer formation.

Experimental determinations of time required for wafer formation, for the bag formation phase to start, and for total breakup of the liquid globule are reported.

A preliminary consideration of the stability of droplets in a low Reynolds number gas flow region ($N_{Re_D} = 10$) indicates that the change of environmental conditions causes specific changes in the critical stability criterion and the time required for deformation of the droplet to the wafer shape.

The model used for deformation has not included the variation of pressure distribution about the globule during the deformation proces. This effect is under investigation.

## ACKNOWLEDGMENT

This work, sponsored by the Sandia Corporation, was performed as part of contract P.O. No. 51-1136. The author thanks the Sandia Corporation and Cornell Aeronautical Laboratory, Inc., for permission to publish this work and acknowledges many useful discussions with Dr. J. L. Beal and Mr. G. A. Sterbutzel of Cornell Aeronautical Laboratory. Mr. A. K. Ashby performed the experimental program, and Mr. G. A. Sterbutzel developed the photographic techniques.

## NOTATION

$D$ = diameter

$N_{Re_D}$ = Reynolds number $= \dfrac{D\,V\,\rho_g}{\mu_g}$

$N_{We}$ = Weber number $= \dfrac{R\,V^2\,\rho_g}{\sigma_l}$

$P$ = pressure

$P_n$ = surface zontal harmonic of order $n$

$R$ = radius of undeformed drop

$t$ = time

$V$ = velocity differential between drop and surroundings

### Greek Letters

$\delta$ = amount of deformation at stagnation point

$\mu$ = viscosity

$\rho$ = density

$\sigma$ = surface tension

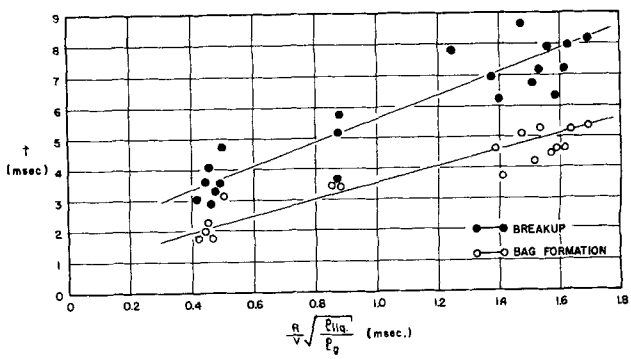


Fig. 8. Experimentally determined times for start of bag formation and complete globule breakup.

$\phi$ = angle measured from stagnation point
$\omega_n$ = defined by Equation (2*a*)

**Subscripts**

$c$ = critical condition
$g$ = gas
$l$ = liquid
$m$ = maximum value
$s$ = stagnation point

**LITERATURE CITED**


1. Hinze, J. O., *A.I.Ch.E. Journal*, **1**, No. 3, p. 289 (1955).
2. ———, *Appl. Sci. Research*, **A1**, 263 (1949).
3. *Ibid.*, p. 273.
4. Dwight, H. B., "Tables of Integrals and Other Mathematical Data," p. 192, Macmillan, New York (1947).
5. Flashsbart, O., *Phys. Z.*, **22**, 461 (1927); also see Schlichting, H., "Boundary Layer Theory," p. 20, McGraw-Hill, New York (1960).
6. Magarvey, R. H., and B. W. Taylor, *J. Appl. Phys.*, **27**, 10 (1956).
7. Merrington, A. C., and E. C. Richardson, *Proc. Phys. Soc.*, **59**, 1 (1947).
8. Jensen, V. G., *Proc. Roy. Soc.*, **A249**, 346 (1959).
9. Homann, F., *Natl. Advisory Comm. Aeronaut. Tech. Memo 1334* (1936).



*Manuscript received November 11, 1963; revision received June 12, 1964; paper accepted June 15, 1964. Paper presented at A.I.Ch.E. Memphis meeting.*


# Solids Mixing in Straight and Tapered Fluidized Beds


**HOWARD LITTMAN**

**Argonne National Laboratory, Lemont, Illinois**


It is generally thought that the solids in a gas fluidized bed mix rapidly and that this mixing is responsible for the desirable properties of fluidized beds, namely good contact between gas and solids, high rates of heat transfer, and temperature uniformity within the bed. But a high solids mixing rate is not always desirable. In the continuous chemical processing of solid materials (particularly where high conversion solid product is required) it is useful to reduce the rate of solids mixing in the longitudinal direction and still retain the desirable properties of the fluidized bed.

Solids mixing is not the only problem, however; deep beds of dense materials do not fluidize well. Levey et al. (3) reported violent bed eruptions and inefficient contacting in a 5-in. diameter bed of 20 to 40 mesh $UO_3$ particles when the static bed heights exceeded 4 diam. He observed that fluidization began at the upper surface of the bed and proceeded downward through the bed as the inlet gas velocity was raised, and when the gas velocity was sufficient to fluidize the bed completely, the upper portion of the bed was slugging.

Since the superficial gas velocity increases considerably along the bed owing to expansion of the gas (the pressure drop in beds of $UO_3$ is approximately 1.75 lb./sq. in./ft.) the bubble volume increases steadily along the bed, and thus the deeper the bed and the higher the particle density the greater the tendency of the bed to slug. To compensate for the gas expansion, Levey et al. tapered the bed to obtain a constant superficial gas velocity along the bed. In this way, solids mixing in the bed was reduced, deep beds of dense materials fluidized better, and both conversion rates and productivity were increased.

According to Romero and Johanson (9), the reduced rate of solids mixing is caused by operating close to the minimum fluidizing velocity (MFV). Sutherland (10) concluded that the effect of tapering is to reduce the vertical mixing rate in deep beds of dense materials. Furthermore, he specified that this effect is confined to beds in which the gas flow rates are less than 30% above the minimum and to bed heights greater than 2 ft. Sutherland found as Levey et al. did that particle movement and bubbling in untapered beds began at the top of the bed as the air rate was increased, and that by the time particle movement was observed at the base, the top was slugging violently. In tapered beds, he observed that the fluidization was more even with bubbles appearing in the lower as well as the upper part of the bed.

In this paper, solids mixing rates are reported for −140 +200 mesh copper particles in straight and tapered fluidized beds of rectangular cross section with a 2-in. sq. inlet. Gas velocities up to 110% above the minimum and bed height to diameter ratios of 8 and 16 to 1 were employed. The object of this work is primarily to compare the rates of solids mixing of dense particles in tapered and untapered beds with high $L/D$ ratios (8 and 16 to 1).

## EQUIPMENT AND MATERIALS

The apparatus consists of a metered air supply, two columns, counting, and recording equipment. A schematic drawing is shown in Figure 1.

The tapered and untapered columns used in this work are 50 in. high and have a 1.992 in. sq. inlet. The outlet for the tapered column is 1.992 × 2.880 in. The untapered column is assembled from four aluminum plates (¼ in. thick) which are gasketed and bolted together. When the tapered column is desired, the front and rear plates of the untapered column are replaced by two tapered plates, each making an angle of 0.509 deg. with the vertical.

The square inlet is bolted into a bottom header into which the metered gas is fed. Separating the gas space of the header from that in the column is a sintered, stainless steel, gas distributor plate. The outlet is fitted with a gas outlet port and a tracer charging mechanism. This mechanism consists of a cylinder, one end of which is soldered to a ⅜-in. hard copper tube and the other is closed by a rubber stopper. The copper tube passes through the top header where it is positioned. The tracer charging cylinder can thus be placed at any level in


Howard Littman is at Syracuse University, Syracuse, New York.